

Prediction of Flow Behaviour in an Axial-To-Radial Diffuser

Abdus Salam*
J. De Ruyck**
Ch. Hirsch***

ABSTRACT :

A three dimensional end-wall boundary layer theory is applied in order to predict the flow behaviour in an axial-to-radial diffuser with inlet swirl .

Boundary layer profiles are predicted and matched with the main inviscid flow, which is determined from a simple radial equilibrium approach where end-wall blockage effects are taken into account.

Complete spanwise three dimensional velocity profiles are calculated and compared with experimental data at several locations in the diffuser, for three different test configurations.

Nomenclature :

Q = volume flow
 A = cross-sectional area
 B = blockage factor
 h = diffuser spacing at exit
 R = radius of curvature
 r = radius
 V_m = meridional velocity
 V_{me} = free stream meridional velocity
 α = inlet flow angle downstream from the guide vanes rings
 β = angle between the meridional plane and velocity vector
 $\epsilon = \beta_\infty - \beta$ = skewing angle of boundary layer
 ϵ_w = wall skewing angle
 m, n, u = in meridional coordinates
 x, y, z = in cartesian coordinates

Subscripts and superscripts

e = external flow
 w = at the wall
 \wedge = inviscid main flow parameter
 \sim = pitch average value

Introduction :

The flow conditions in a diffuser are in general critical and as a consequence, diffusers are often a delicate part of a fluid flow system. Reliable diffuser flow prediction methods are, therefore, important whereas such methods are not profuse due to the near stall flow conditions.

*Graduate Student
**Research Assistant
***Professor

Department of Fluid Mechanics
VRIJE Universiteit Brussel, Pleinlaan-2, 1050 Brussels, Belgium.

The choice of a diffuser is in general based on experimental characteristics which are available in the literature (1, 2). Simple conical, rectangular and annular diffusers are quite well designed in this way, whereas the effects of inlet swirl, inlet blockage and wall curvature are less clear at the present time.

In the present paper, the flow behaviour in an axial-to-radial diffuser with inlet swirl is predicted by use of a three dimensional end-wall boundary layer prediction method which interacts with a simple radial equilibrium approach.

Experimental data are available from MIT(3). Several test configurations are available, obtained through the variation of the axial distance h between the two diffuser walls (fig. 1)

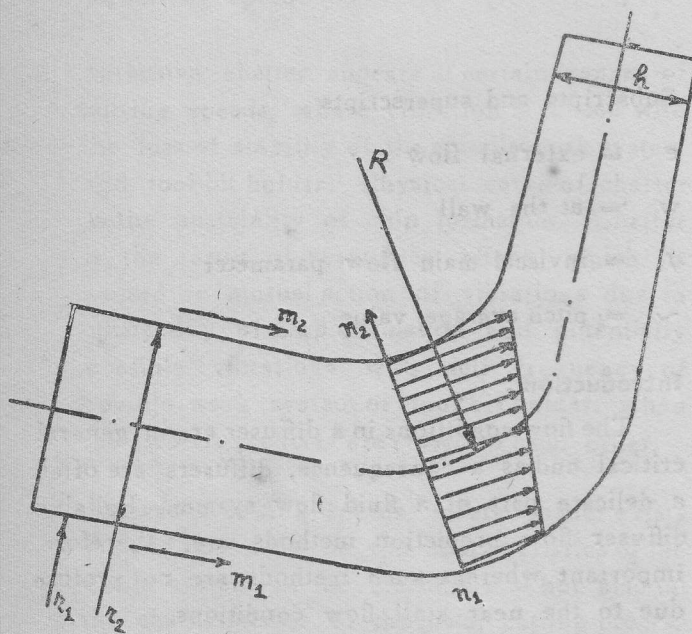


Fig. 1

Increasing, decreasing and nearly constant cross sections are obtained in this way.

The end-wall boundary layer calculation is described in De Ruyck and Ch. Hirshch (4-7). This method consists of a three dimensional integral boundary layer approach, where boundary layer velocity profiles are reconstructed through the use of velocity profile models.

The mainflow is predicted from a simple radial equilibrium approach where the end-wall blockage is taken into account.

Complete velocity profiles are reconstructed and compared with experimental data at seven locations inside the diffuser, for three test configurations, an increasing, decreasing and nearly constant cross-section test cases.

1. END-WALL BOUNDARY LAYER THEORY

1. Basic Equations: In the present section, the end-wall boundary layer theory as presented in (4-7) is briefly summarized.

The basic equations are written as follows:

$$\frac{d}{dm} r_0 \rho_0 V m^2 \theta_{mm} + r_0 \rho_0 V m_0 \delta^* m \frac{dV m_0}{dm} - \rho V m^2 \text{Sin} \alpha$$

$$(\delta^*_{ut} g \alpha + \theta_{uu}) = r_0 \tau_{wm} \dots \dots \dots (1)$$

$$\frac{d}{dm} r_0 \rho_0 V m^2 \theta_{um} + r_0 \rho_0 V m_0 \delta^* m \frac{dV u_0}{dm} + \rho V m^2 \text{Sin} \alpha$$

$$(\delta^*_{mt} g \alpha + \theta_{um}) = r_0 \tau_{wu} \dots \dots \dots (2)$$

A coordinate system denoted as meridional coordinate system is used. The corresponding coordinates are m, n, u where m denotes the meridional direction, n the direction normal to the end wall and u is the pitchwise direction (fig.1).

Equations 1 and 2 are valid for an axisymmetric flow. In the case of non-axisymmetric flows (such as turbomachine flow), extra terms denoted as 'defect forces' are to be added.

1.2 Introduction of Complementary Relations: In the above equations six unknowns appear: θ_{mm} , θ_{um} , θ_{uu} , $\delta^* m$, τ_m , τ_u . Only two equations are available through eqs. 1 and 2 and therefore additional relations are searched. Heads entrainment equation is given by

$$\frac{d}{dm} (\delta - \delta^*_{m}) = \frac{F(H^*)}{\cos \alpha} - (\delta - \delta^*_{m}) \frac{1}{V} \frac{dv}{dm} \dots \dots (3)$$

The estimation of the mainstream skin friction occurs through the use of a non-dimensional skin friction coefficient generally noted as C_f . The popular relation for C_f is probably the Ludwig Tillman's relation which is generally accepted.

$$C_f = .246 \text{Re}(\theta_m)^{-.268} \exp(-1.56H) \dots \dots (4)$$

Where $\text{Re}(\theta_m)$ is defined by

$$\text{Re}(\theta_m) = \frac{V_{me} \theta_m}{\nu} \dots \dots (5)$$

1.3 Velocity Profile Models: Kool's [8] profile model, which is adapted for turbomachinery application is used to construct the velocity profile. The proposed model in meridional direction is as follows:

$$\frac{V_m}{V_{me}} = 1 - b(1 - y')^n \dots \dots (6)$$

Where $y' = y/\delta$, b is the velocity defect at the edge of the small inner layer, and n is the velocity profile model power. 'b' is related to the skin friction through.

$$b = \exp(-7nC_f \cos \alpha^{-.134}) \dots \dots (7)$$

2. THE MAIN FLOW PREDICTION: Main flow quantities are denoted with an overhead carat ($\hat{}$) and are to be considered as inviscid. Two quantities V_m and V_u are to be determined to construct the velocity profile through the axial to radial diffuser. Throughout the pure axial radial part of the diffuser, the mainflow velocity remains uniform over the span of the diffuser. In the curved portion of the diffuser the velocity profile is not uniform.

2.1 Meridional Velocity Prediction: According to the continuity the span average meridional velocity V_m is determined through

$$V_m = Q/S(1-B) \dots \dots (8)$$

Where Q = Volume flow

S = area of cross-section

B = blockage

The average meridional velocity, V_m is found at each section as function of the blockage, B which is to be determined through end-wall boundary layer theory. The non-uniformity of V_m will be determined through continuity and the circumferential velocity will be determined through radial equilibrium.

The angular velocity is given by

$$W_u = \frac{\delta V_m}{\delta n} + \frac{V_m}{R} - \frac{\delta V_n}{\delta V_m} = 0 \dots \dots (9)$$

The velocity normal to the wall V_n is very small in comparison to the meridional velocity. Therefore, the third term on the left hand side of the equation can be neglected. After integrating eq. (9) from the lower wall till the upper wall (n_1, n_2) following expression can be found,

$$\hat{V}_{m2} - \hat{V}_{m1} = \bar{V}_m / R \cdot h \dots \dots (10)$$

It will be assumed that \hat{V}_m varies in a linear way over the diffuser span. From the results this assumption seems to give a satisfactory approach for the present tests.

$$V_{m2} = V_m + (V_m/R)h/2 \dots \dots (11)$$

$$V_{m1} = V_m - (V_m/R)h/2 \dots \dots (12)$$

and \hat{V}_m is given by

$$\hat{V}_m = \hat{V}_{m1} + (\hat{V}_{m2} - \hat{V}_{m1})n/h \dots \dots (13)$$

If the average meridional velocity (\bar{V}_m) is known at a particular section, the velocities (V_{m1}, V_{m2}) at both upper and lower walls can be determined using eqs (11) and (12), V_m follows from eq (13).

2.2 Circumferential Velocity Prediction: The circumferential velocity is calculated by radial equilibrium which in the present case reduces to

$$R \cdot \hat{V}_u = \text{cte}, \dots \dots (14)$$

3. Viscous-Inviscid Intereaction: The viscous and inviscid parts of the flow interact through a simple iterative procedure. The inviscid flow is searched through equations (8), (13) and (14)

assuming an arbitrary initial blockage B. The end-wall boundary layer theory is applied using eqs (1) to (8), giving a new blockage distribution and a inviscid flow field.

This procedure is repeated until a constant blockage is found. The 'main flow' velocities in eqs (1) to (8) are taken at the walls (\hat{V}_{m1} , \hat{V}_{m2} , \hat{V}_{u1} , \hat{V}_{u2}) (4).

3.1 Matching of the velocity profiles: In order to construct complete spanwise profiles \hat{V}_m and \hat{V}_u are to be matched, the matching of the profile model and the mainflow profile (\hat{V}) is done by matching the profiles at the boundaries $n = 0$ and $n = \delta$. This can be done by setting (fig 2).

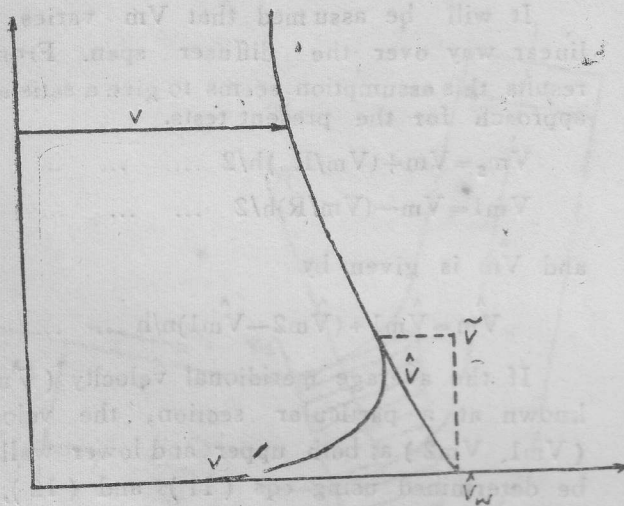


Fig. 2

$$\hat{V} - V_{real} = \hat{V}_w - V$$

or $V_{real} = \hat{V} + \hat{V} - \hat{V}_w \dots (15)$

4. Comparison with experimental data:

From the report of Drum (3) data were available for six geometrical configurations (3 increasing, 2 nearly constant and 1 decreasing area). The configurations are identified by a

run number. For each configurations seven stations along the diffuser had been taken into consideration and at each station the velocity magnitude and the flow angle β were measured at several points from the lower wall.

Out of six configurations three have been selected: one increasing, one nearly constant and one decreasing area (RUN A.E. & F.)

To start the calculation only the experimental inlet conditions V_m , V_u , the profile model power n , the skin friction and the wall skewing angle are needed.

The start values of n , cf and ϵ_w were obtained through a fit of the profile model equations with the experimental profiles at the first station.

MIT AXIAL TO RADIAL DIFFUSER
INCREASING AREA

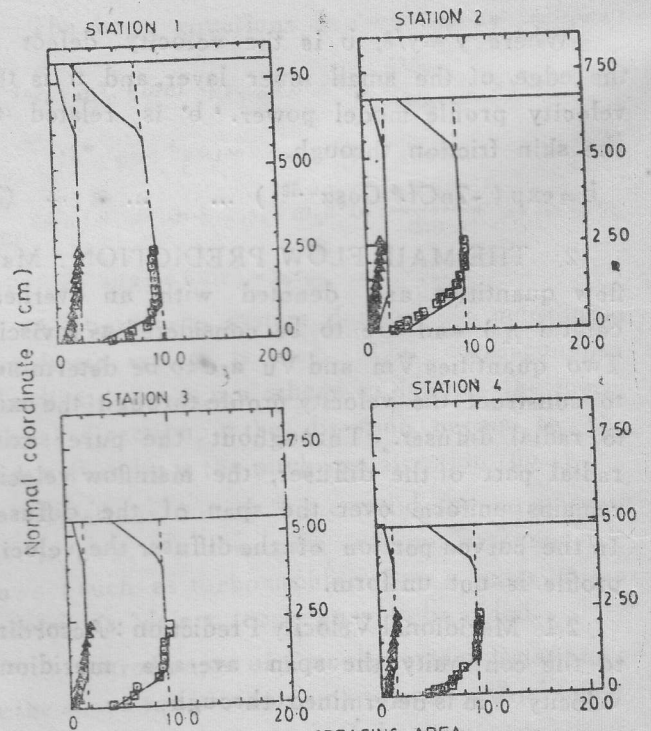


FIGURE 3 INCREASING AREA
SOLID LINE CALCULATED
□ EXP MERID VELOCITY
▲ EXP CIRC VELOCITY
Merid and circumf velocity (m/s)

Since the geometry of the diffuser is not clearly defined in (3) some problems arose in defining the correct height h at each station. The height of a particular section is corrected by adjusting the total mass flow rate through the section.

5. Summary of Results :

The results are shown in figures 3 to 5. In each figure, a comparison is made between the experimental and calculated profile of \hat{V}_m and \hat{V}_u . The profiles \hat{V}_m and \hat{V}_u moreover are extended up to the end-walls. No experimental data are available in the axial part of the diffuser. Stations 1 to 3 are inside the curved portion of the diffuser and the non-uniformity of the main velocity \hat{V} can clearly be seen. The remaining stations are in the pure radial part.

M. I. T. AXIAL TO RADIAL DIFFUSER CONSTANT AREA

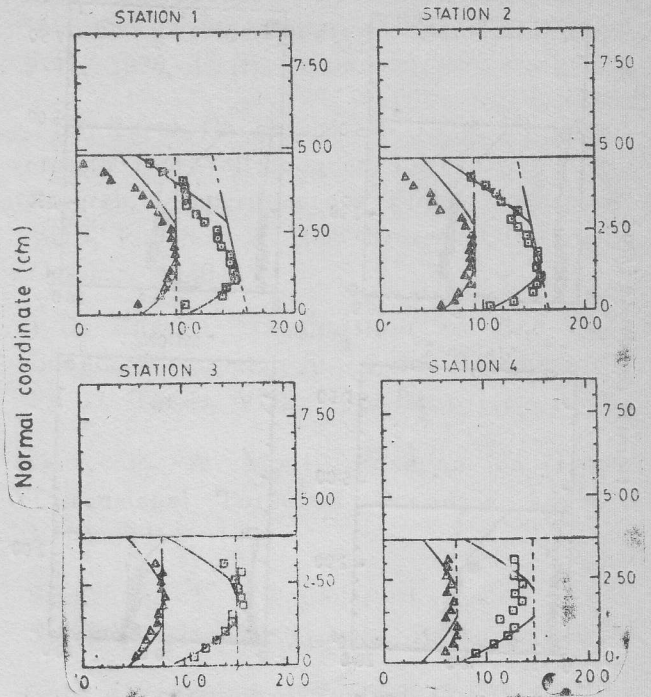


FIGURE 4

CONSTANT AREA
SOLID LINE CALCULATED
□ EXP. MERID. VELOCITY
▲ EXP. CIRC. VELOCITY

Merid and circumf. velocity (m/s)

M. I. T. AXIAL TO RADIAL DIFFUSER CONSTANT AREA

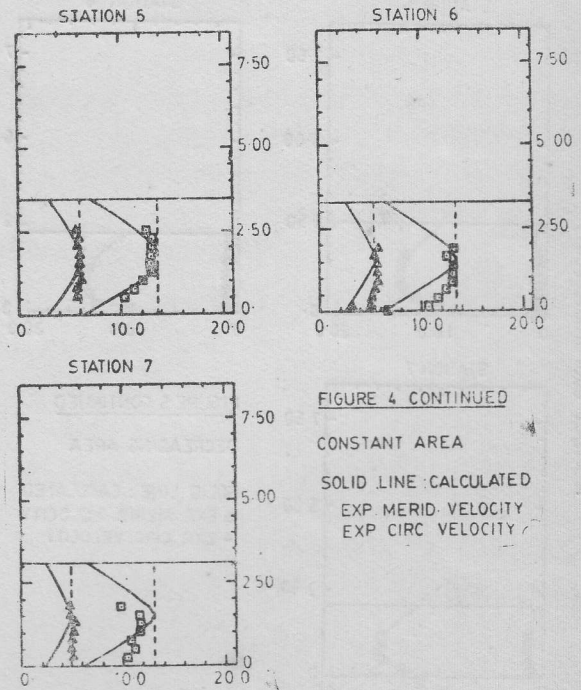


FIGURE 4 CONTINUED

CONSTANT AREA
SOLID LINE CALCULATED
EXP. MERID. VELOCITY
EXP. CIRC. VELOCITY

Merid. and circumf. velocity (m/s)

M. I. T. AXIAL TO RADIAL DIFFUSER- INCREASING AREA

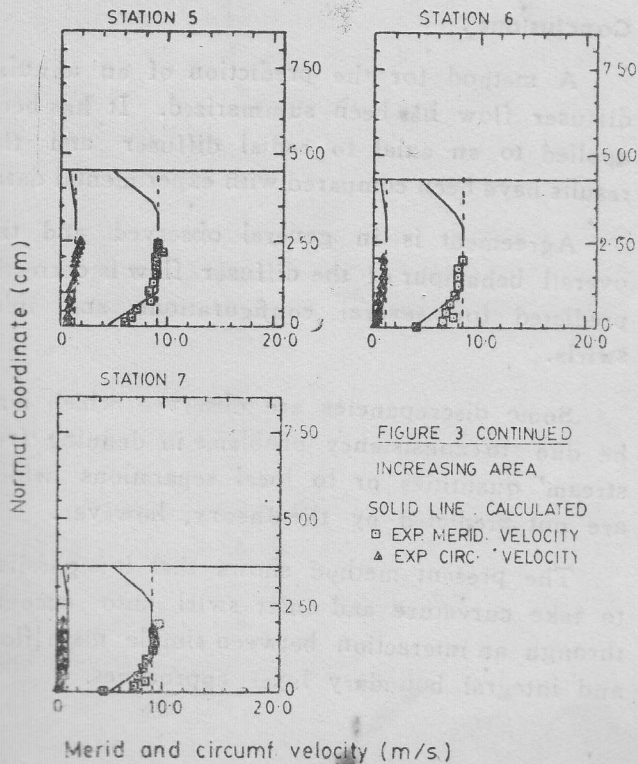


FIGURE 3 CONTINUED

INCREASING AREA
SOLID LINE CALCULATED
□ EXP. MERID. VELOCITY
▲ EXP. CIRC. VELOCITY

Merid and circumf. velocity (m/s)

M. I. T. AXIAL TO RADIAL DIFFUSER
DECREASING AREA

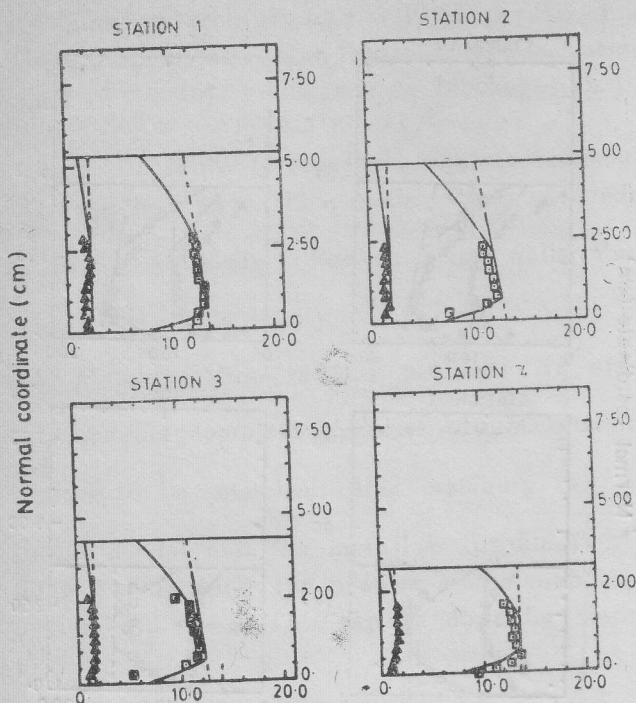


FIGURE 5
DECREASING AREA
SOLID LINE CALCULATED
□ EXP. MERID. VELOCITY
▲ EXP. CIRC. VELOCITY

Merid. and circumf. velocity (m/s)

M. I. T. AXIAL TO RADIAL DIFFUSER
DECREASING AREA

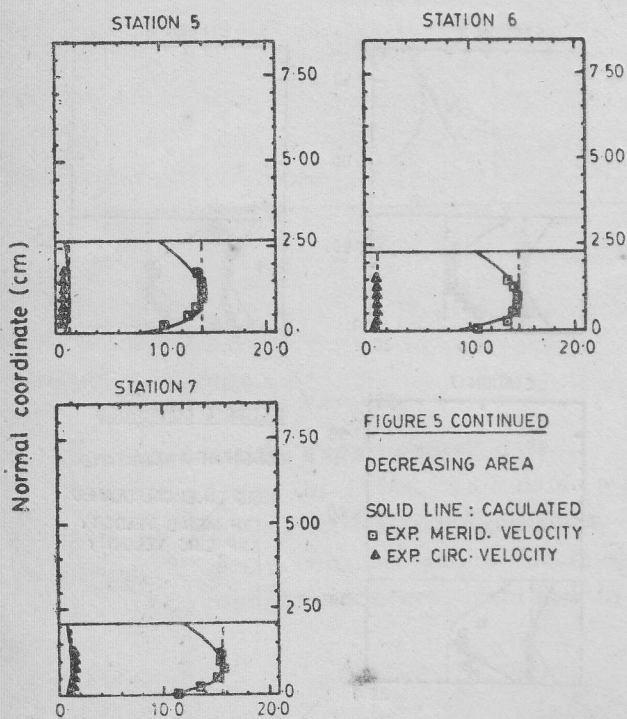


FIGURE 5 CONTINUED
DECREASING AREA
SOLID LINE : CALCULATED
□ EXP. MERID. VELOCITY
▲ EXP. CIRC. VELOCITY

Merid. and circumf. velocity (m/s)

5.1 RUNJA (inlet swirl 23 degrees, increasing area): Figure 3 it can be seen that the predicted velocity profiles compare well with the measured profiles, although the pressure gradient is the most adverse one and the blockage is the thickest one, when compared with the other runs. The freestream velocity should normally decrease from inlet to the outlet (increasing area), but this is not the case due to the increasing end-wall blockage effects.

5.2 RUNE (nearly constant area, inlet swirl 59 degrees). The blockage levels are however, in general well predicted in all the stations (V_m profiles).

In the large inlet swirl case, a good agreement is observed up to station 4, although a very large inlet blockage is present (fig. 4, station 1). At exit the boundary layers are almost confluent.

5.3 RUN F (decreasing area): From figure 5 it appears that in case of decreasing area a fair agreement with the experimental data is found. The pressure gradient is negative, the inlet swirl is small and the experimental data are of good quality.

Conclusions :

A method for the prediction of an annular diffuser flow has been summarized. It has been applied to an axial to radial diffuser and the results have been compared with experimental data.

Agreement is in general observed and the overall behaviour of the diffuser flow is correctly predicted for several configurations and inlet swirls.

Some discrepancies are observed which may be due to consistency problems in defining 'free stream' quantities or to local separations which are not predicted by the theory, however.

The present method shows that it is possible to take curvature and inlet swirl into account through an interaction between simple main flow and integral boundary layer approaches.

References :

1. G. Sovran, D. Klomp : "Experimentally Determined Optimum Geometries for Rectilinear Diffusers with Conical or Annular Cross-Section" General Motors Research Laboratories, Warren, Michigan.
2. A. Klen, 'REVIEW' : "Effects of Inlet Conditions on Conical-Diffuser Performance" ASME Transaction, Journal of Fluids Engineering, Vol. 103, 1981.
3. N. J. Drum : "Investigation of the Flow in an Axial to Radial Diffuser" MIT, USA, October, 1971.
4. J. De Ruyck, Ch. Hirsch, P. Kool : "An Axial Compressor End-Wall Boundary Layer Calculation Method", ASME Transaction 1978.
5. J. De Ruyck, Ch. Hirsch, P. Kool : "Investigation on Axial Compressor End-Wall Boundary Layer Calculation" The 1979 International Joint Gas Turbine Congress & Exhibition, July 9-11, 1976, Haifa, Israel.
6. J. De Ruyck, Ch. Hirsh : "VUB Axial Compressor End-Wall Boundary Layer Calculation Program" Department of Fluid Mechanics, VUB, Pleinlaan-2, 1050 Brussels. Reviewed, October, 1980.
7. J. De Ruyck : "Computation of End-Wall Boundary Layers in Axial Compressor" Ph. D. Thesis, VUB, 1981-82.
8. Kool, P. "A Model Equation for Three Dimensional Turbulent Boundary Layer." VUB-STR-6, 1979.
9. Schlichting, H, "Boundary Layer Theory" Seventh edition, Mc. Grawhill Book Company.
10. G N. Abramovitch, "Applied Gas Dynamics" 3rd edition of <<NAUKA>> Moscow, 1969.